Liquid-Liquid Phase Transition: Evidence from Simulations

Stephen Harrington,[1] Rong Zhang,[1] Peter H. Poole,[2] Francesco Sciortino,[3] and H. Eugene Stanley[1]
[1]*Center for Polymer Studies and Department of Physics, Boston University, Boston, Massachusetts 02215*
[2]*Department of Applied Mathematics, University of Western Ontario, London, Ontario, Canada N6A 5B7*
[3]*Dipartimento di Fisica and Istituto Nazionale per la Fisica della Materia, Universita' di Roma La Sapienza, Piazzale Aldo Moro 2, I-00185, Roma, Italy*
(Received 20 December 1996)

We report, using extensive molecular dynamics simulations of a one-component model system, a first-order liquid-liquid phase transition. Specifically, by evaluating the pressure-density isotherms above and below a critical temperature, we find the presence of two coexisting phases differing by ~15% in density. Moreover, system points in an unstable region decompose into two different spatially separated phases. We identify the two phases, characterized by different local structures and local dynamics, by studying the static structure factor $S(q)$ at small wave vector q. [S0031-9007(97)02805-6]

PACS numbers: 64.70.Ja, 61.20.Ja

There is increasing interest in the properties of network-forming liquids at low temperatures [1]. In the case of water, several studies [2–8] are germane to the hypothesis [2] that in addition to the known critical point C, a *second* critical point C' might possibly occur at low temperature T [9]. Despite these studies, the evidence supporting the possibility of a liquid-liquid critical point in a one-component system is not conclusive. In this Letter, we report an extensive evaluation of the equilibrium equation of state and structure factor obtained from molecular dynamics (MD) simulations of a system of 1728 molecules which interact through the ST2 potential [10,11]. To obtain high-quality statistics, we perform five to eight *independent* simulations for each state point (see Table I). Compared to previous studies [2], the numerical error is decreased by a factor of 10, allowing for a precise determination of the low T equation of state. We find that in this one-component liquid model, a transition exists between two distinct liquid phases that differ in density, and therefore support the hypothesis of a liquid-liquid critical point.

In Fig. 1(a), we show equilibrium isotherms of pressure P as a function of density, ρ, for three different temperatures, $T = 290$, 250, and 235 K. The local slopes are calculated by determining the structure factor, $S(q)$, and using the relation $K_T = \rho kTS(0)$, where $K_T \equiv \rho^{-1}(\partial\rho/\partial P)_T$ is the isothermal compressibility and k Boltzmann's constant. Note that on decreasing T, an inflection develops. At $T = 235$ K, we see from Fig. 1(b) that P does not increase over a range of ~15% in ρ, providing evidence outside the numerical error for the existence of a first-order transition between two liquids. We note that the density difference in the coexistence region coincides with systems of 216 molecules [2].

The three simulated state points in the unstable region, at $\rho = 0.975$, 1.00, and 1.025 g/cm^3 for $T = 235$ K, undergo phase separation during the equilibration process, and show a marked increase in $S(q)$ at very small q [Fig. 2(a)]. Our simulations show that the system separates into two coexisting phases separated by an interface. Mass conservation fixes the relative amount of the two different phases. The two coexisting phases are in dynamic equilibrium so molecules exchange between phases over time. To identify the composition and structure of each phase, we separate molecules into two groups according to the number of neighbors n_{OO} within 0.34 nm of each molecule, averaged over a time of 200 ps [15]. During 200 ps, molecules diffuse less than one molecular diameter, a distance much smaller than the characteristic size of each of the two coexisting phases. As a classification

TABLE I. Properties of simulated state points. U is the configurational part of the internal energy, D the diffusivity, and N_{runs} is the number of independent runs carried out for each state point. The statistical error for U is less than 0.01 kJ/mol for all points. The $T = 235$ K simulations are for 1 ns after equilibrium, except for the $\rho = 1.00$ g/cm^3 which was run for 1.5 ns. The higher T simulations are fun for 200 ps for equilibration and then for an additional 400 ps to evaluate the quantities reported here.

T (K)	ρ (g/cm^3)	P (MPa)	U kJ/mol	D (10^{-5} cm^2/s)	N_{runs}
235	0.900	183 ± 9	−43.66	0.02 ± 0.005	1
235	0.925	219 ± 3	−43.19	0.03 ± 0.005	5
235	0.950	231 ± 2	−42.66	0.06 ± 0.007	7
235	0.975	221 ± 3	−42.06	0.10 ± 0.008	5
235	1.000	223 ± 2	−41.65	0.14 ± 0.008	8
235	1.025	225 ± 2	−41.28	0.18 ± 0.01	5
235	1.075	229 ± 3	−40.63	0.27 ± 0.01	5
235	1.100	241 ± 2	−40.44	0.30 ± 0.02	8
250	0.925	129 ± 4	−41.03	0.12 ± 0.01	5
250	0.975	163 ± 4	−40.19	0.29 ± 0.01	5
250	1.025	182 ± 4	−39.45	0.45 ± 0.02	5
250	1.075	210 ± 5	−38.99	0.60 ± 0.03	5
290	0.925	23 ± 2	−35.92		5
290	0.975	75 ± 3	−35.54		5
290	1.025	129 ± 3	−35.25		5
290	1.075	195 ± 3	−35.07		5

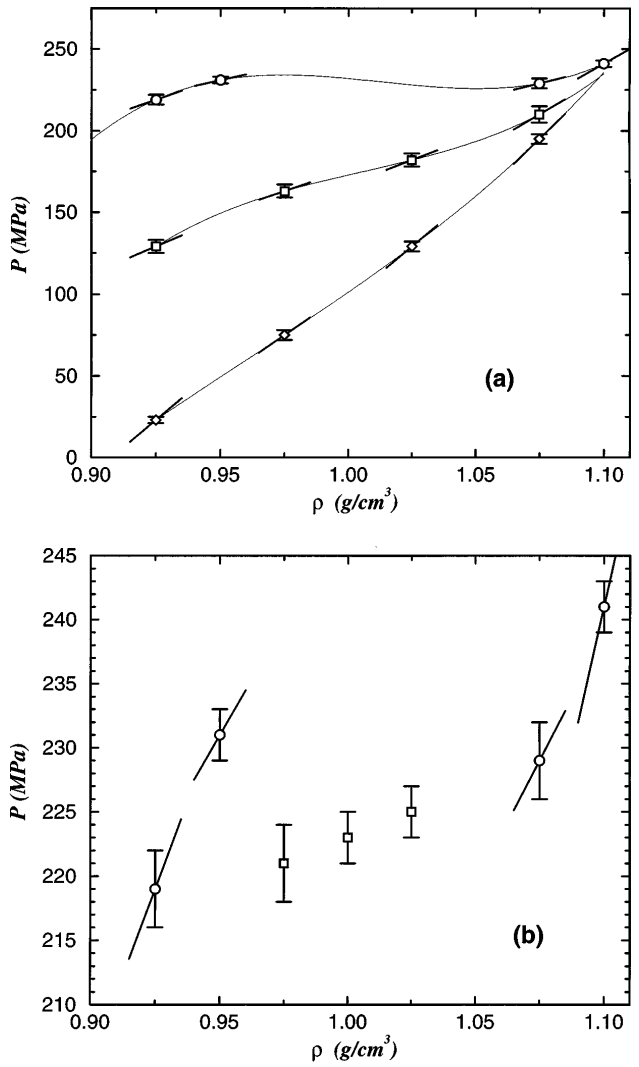

FIG. 1. (a) P-ρ isotherms for $T = 290$ K ($\diamond$), $T = 250$ K ($\square$), $T = 235$ K ($\circ$). The local slopes (heavy line segments) are calculated from the extrapolated $q \to 0$ values of $S(q)$—a 10% error is made in determining $S(0)$. Error bars for P are calculated from averages over independent time intervals and independent samples. Also shown (light line) is a spline fit between the state points. (b) Detail of 235 K isotherm, showing the three state points within the coexistence region ($\square$). Note that $P(\rho = 0.95\ \mathrm{g/cm^3}) > P(\rho = 0.975\ \mathrm{g/cm^3})$, well outside the numerical error.

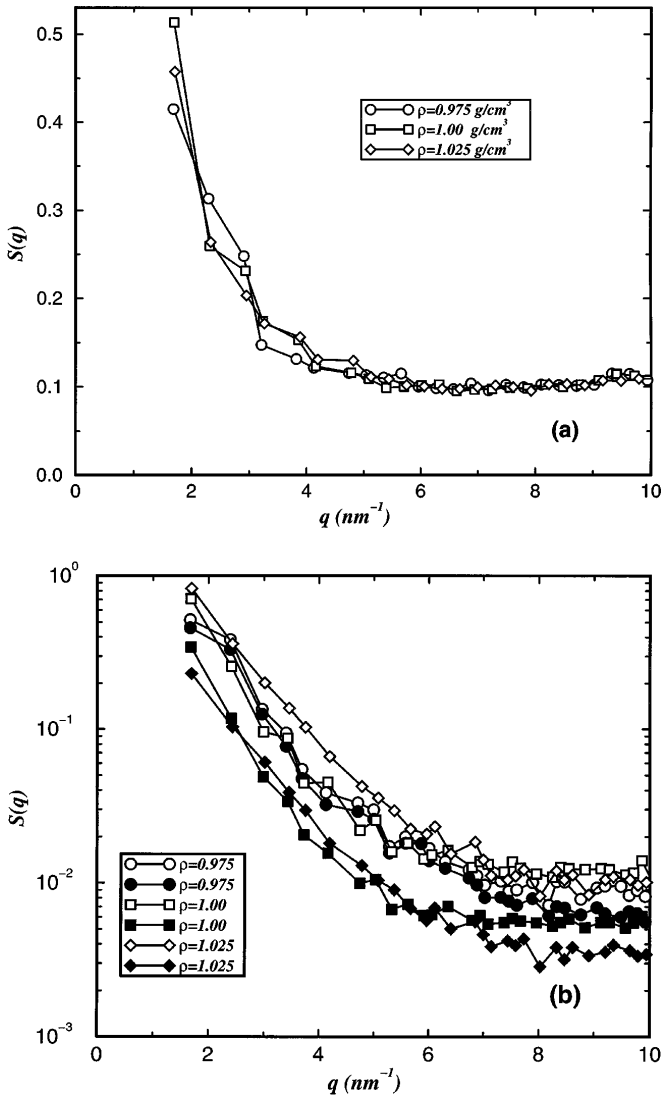

FIG. 2. (a) Small q static structure factor, $S(q)$, for the three samples within the unstable region at $T = 235$ K. Note the significant scattering at q of the order of the inverse of the system size. (b) Semi-log plot of $S(q)$ evaluated for each of the two coexisting phases at $T = 235$ K and $\rho = 0.975$, 1.00, and 1.025 g/cm^3. The open symbols represent the low-density phase and the filled symbols the high-density phase. Note that the small q scattering for each of the two phases is consistent with the $S(q)$ of the entire system, supporting the identification of the increase in $S(q)$ with the presence of phase separation.

criterion, we say that molecules with $n_{OO} < 4.4$ are in the low-density liquid phase, and molecules with $n_{OO} \geq 4.4$ are in the high-density liquid phase [16].

To assess the spatial arrangement of these two groups and to support the choice of the classification criterion, we evaluate $S(q)$ for each of the two groups of molecules. We find [Fig. 2(b)] that $S(q)$ for each group has a strong q dependence at small q, confirming the presence of spatial correlations among molecules in each group. $S(q)$ for each of the two groups decreases by more than 2 orders of magnitude from $q = 2.0$ to $q = 6.0$ nm^{-1}, suggesting that the size of the correlated region is comparable to the size of the simulated system. Moreover, the values of q for which there is an increase in $S(q)$ for each group is the same range in q where $S(q)$ for the entire system increases, supporting the hypothesis that the two groups of molecules offer a correct description of the two phases.

To better visualize the phase-separated structure, we show in Fig. 3 the spatial arrangement of the low- and high-density phases for several densities along the $T = 235$ K isotherm. Visual inspection confirms that the metastable state with $\rho = 0.95$ g/cm^3 is indeed a homogeneous single phase, while the three states in

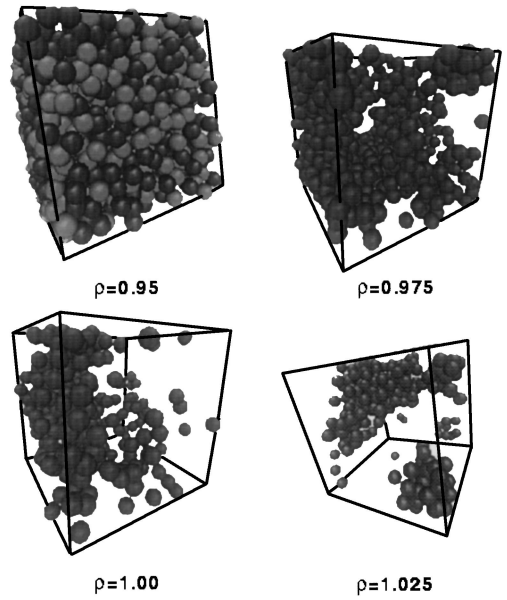

FIG. 3. Snapshots of the MD configuration after 1 ns for selected densities spanning the coexistence region at $T = 235$ K. For clarity, only the oxygen atom on each water molecule is shown. Molecules of the high-density phase are lightly shaded, molecules of the low-density phase are dark. For the three state points within the coexistence region, we show only the low-density molecules to highlight the presence of the two coexisting phases. Note that the state point $\rho = 0.95$ g/cm^3 does not show significant space correlation.

the unstable region ($\rho = 0.975$, 1.00, and 1.025 g/cm^3) display two separated phases.

We find that the first-order transition is between two *liquid* phases [17]. State points on the two sides of the coexistence region exhibit diffusivities differing by an order of magnitude. In contrast to simple liquids, the high density phase, $\rho \geq 1.075$ g/cm^3, is characterized by higher molecular mobility [18]. Interestingly, the diffusivity of the two groups of molecules, identified for $\rho = 0.975$ g/cm^3, differs by a factor of 6 over a time of 500 ps.

Next we discuss the change in the n_{OO} distribution, $p(n_{OO})$, as ρ increases along the $T = 235$ K [Fig. 4(a)] and $T = 290$ K isotherms [Fig. 4(a) inset]. (i) For state points along the $T = 290$ K isotherm, $p(n_{OO})$ is always unimodal with a value of average n_{OO} that increases monotonically with ρ. (ii) For state points along the $T = 235$ K isotherm and *outside* the coexistence region, $p(n_{OO})$ is unimodal. On the low-density side of the unstable region, the distribution is highly asymmetric and exhibits an exponential tail. (iii) For state points along the $T = 235$ K isotherm and *inside* the coexistence region $p(n_{OO})$ becomes bimodal, reflecting the fact that there are two underlying distributions representing each of the two phases that are present in the phase-separated system. Moreover, a weighted linear superposition of $p(n_{OO})$ describing the states at either end of the coexistence region

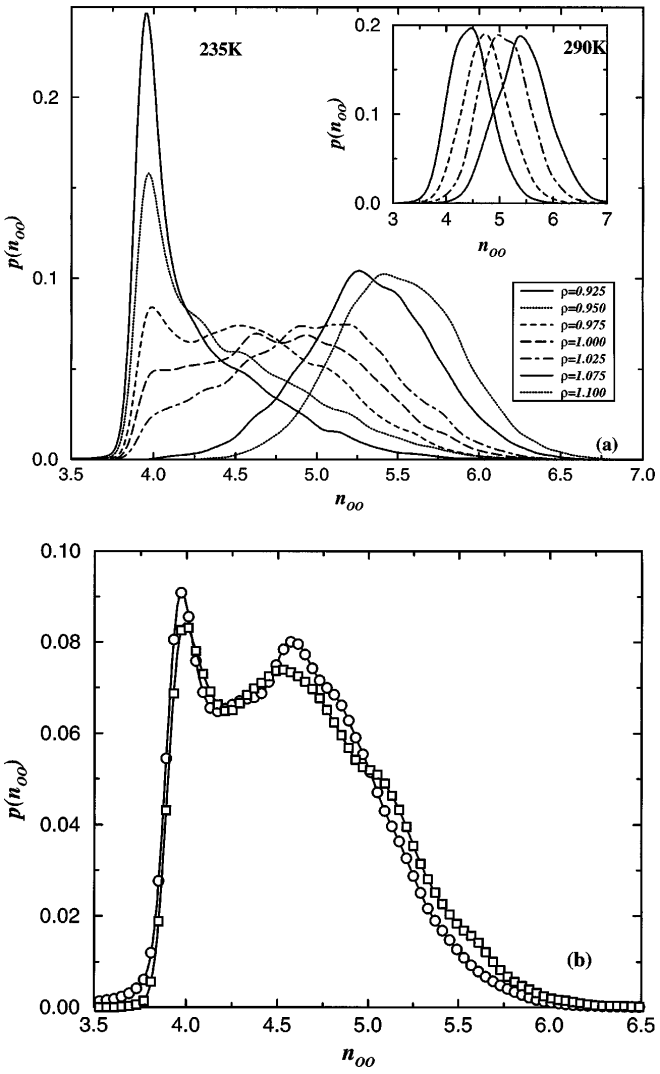

FIG. 4. (a) Distribution, $p(n_{OO})$, of the coordination number, n_{OO}, at $T = 235$ K. The curves for $p(n_{OO})$ are smoothed by averaging over adjacent bins with bin size 0.01. Note that for $\rho = 0.925$ g/cm^3, $p(n_{OO})$ is sharply peaked around $n_{OO} \approx 4$ with an exponentially decreasing tail, while at $\rho = 1.10$ g/cm^3 the distribution is unimodal. For 0.95 g/cm^3 $< \rho <$ 1.075 g/cm^3; $p(n_{OO})$ is not singly peaked about any one value, suggesting more than one underlying distribution. Inset: $p(n_{OO})$ for the 290 K isotherm. Note the unimodal distributions for each density. (b) Linear superposition of $p(n_{OO})$ for equal weightings of $\rho = 0.95$ g/cm^3 and $\rho = 1.075$ g/cm^3. For the purpose of this superposition $p(n_{OO})$, for $\rho = 1.075$ g/cm^3, is shifted to lower n_{OO} values by 0.60 to bring the distribution, $p(n_{OO})$, to its estimated form at the high-density side of the coexistence region. The (○) symbol is $p(n_{OO})$ for $\rho = 0.975$ g/cm^3 from (a) and the (□) symbol is the linear superposition. The close fit is consistent with an underlying phase separated system.

reproduces the bimodal distribution of the phase separated states inside the coexistence region [Fig. 4(b)] [19].

In summary, we have established the existence of a liquid-liquid phase transition in the one-component ST2 model of liquid water and that state points inside the coexistence region evolve in time and separate into two

phases characterized by different densities, structures, and mobilities.

We thank L. A. N. Amaral, C. A. Angell, S. V. Buldyrev, S. Havlin, P. Madden, and R. Sadr-Lahijany for helpful discussions and the Boston University Center for Computational Science for the use of a 32-node SGI Origin2000. Some simulations were carried out at the Maui High Performance Computing Center. S. H. is supported by an NIH fellowship and P. H. P. acknowledges the support of the NSERC (Canada). The Center for Polymer Studies is supported by the NSF and BP.

[1] For reviews, see P. G. Debenedetti, *Metastable Liquids* (Princeton Univ. Press, Princeton, 1997); C. A. Angell, Science **267**, 1924 (1995).

[2] P. H. Poole, F. Sciortino, U. Essmann, and H. E. Stanley, Nature (London) **360**, 324 (1992); F. Sciortino, P. H. Poole, U. Essmann, and H. E. Stanley, Phys. Rev. E **55**, 727 (1997).

[3] Y. Xie, K. F. Ludwig, Jr., G. Morales, D. E. Hare, and C. M. Sorensen, Phys. Rev. Lett. **71**, 2050 (1993).

[4] O. Mishima, J. Chem. Phys. **100**, 5910 (1994).

[5] M. C. Bellissent-Funel and L. Bosio, J. Chem. Phys. **102**, 3727 (1995).

[6] H. Tanaka, Nature (London) **380**, 328 (1996).

[7] S. S. Borick, P. G. Debenedetti, and S. Sastry, J. Phys. Chem. **99**, 3781 (1995); C. J. Roberts, A. Z. Pangiotopoulos, and P. G. Debenedetti, Phys. Rev. Lett. **77**, 4386 (1996).

[8] A. C. Mitus, A. Z. Patashinskii, and B. I. Shumilo, Phys. Lett. **113A**, 41 (1985); S. Aasland and P. F. McMillan, Nature (London) **369**, 633 (1994).

[9] C' is the terminus of a line of first-order phase transitions separating two liquid phases differing in density.

[10] The ST2 model overemphasizes water structure and shifts the phase diagram to higher temperatures and pressures relative to water, yet is an appropriate model for studying supercooled liquids because of relatively short equilibration time scales due to high mobility and the fact that the phase space in the supercooled region has been extensively mapped.

[11] We employ the (N, V, T) ensemble (V is the volume) starting by melting a cubic ice configuration at 600 K and then lowering T to 310 K using a Berendsen rescaling of the velocities with a relaxation time of 10 ps [12]. Coulombic interactions are implemented using the reaction field method with a cutoff of 0.78 nm. Equations of motion are solved using a velocity Verlet update with a time step of 1 fs [13,14]. We prepare ensembles of five to eight independent runs for each state point. We allow the system to equilibrate for 150–200 ps, and then obtain successively lower T by rescaling the velocities in the same manner as above. We confirm that equilibrium is attained when quantities, such as P or potential energy, fluctuate about some average value that is independent of the block sampled. We also confirm that $\langle r^2(t)\rangle$ vs t is linear on a linear scale and $\langle r^2\rangle$ attains a value greater than one molecular diameter ($\sim$0.3 nm) over the course of the equilibration period. For each state point (T, ρ), we calculate P for the system every 0.1 ps for 500–1500 ps after equilibration. The simulation time for all state points recorded in Table I is $\sim$75 ns with simulation speeds of $\sim$60 μs/particle update, for a total of 375 CPU days of computation.

[12] H. J. C. Berendsen, J. P. M. Postma, W. F. Van Gunsteren, A. Dinola, and J. R. Haak, J. Chem. Phys. **81**, 3684 (1984).

[13] O. Steinhauser, Mol. Phys. **45**, 335 (1982).

[14] M. P. Allen and D. J. Tildesley, *Computer Simulation of Liquids* (Oxford University Press, Oxford, 1989).

[15] $r_{\min}$, commonly used to define the first neighbor shell, is the distance coincident with the first minimum in the O-O radial distribution function, $g(r)$; here $r_{\min} = 0.34$ nm.

[16] The coordination number, n_{OO}^i, for each molecule i is a time average of each molecule's O-O radial distribution function, $g^i(r)$, $n_{OO}^i \equiv 4\pi/V \int_0^{r_{\min}} dr\, r^2 \int_0^t g^i(r, t')\, dt'$. Averages over different time intervals modify the distribution of nearest neighbors and introduce an additional parameter in the molecular partitioning, yet we find that the behavior of $p(n_{OO}^i)$ values for the specific choice $r_{\min} = 0.34$ nm, and using an averaging time of 200 ps provides (of all parameter choices examined), the best support for the classification criterion [Fig. 4(a)].

[17] By calculating the $g(r)$ functions along the isotherm, we confirm that only short range order is present, and that crystalization has not occurred in any of the simulated systems.

[18] F. Sciortino, A. Geiger, and H. E. Stanley, Nature (London) **354**, 218 (1991).

[19] Systems with densities in the coexistence region can be considered as mixtures of the two state points at the extrema of the coexistence region only when surface effects are negligible. The choice of $n_{OO} = 4.4$ for the classification criterion is motivated by the minimum of $p(n_{OO})$ at $\rho = 0.975$ g/cm^3.